Journal of Biomolecular NMR, 8 (1996) 252–260
ESCOM

J-Bio NMR 371

Selectively ^{13}C-enriched DNA: Evidence from ^{13}C1' relaxation rate measurements of an internal dynamics sequence effect in the *lac* operator

Françoise Paquet, Florence Gaudin and Gérard Lancelot*

Centre de Biophysique Moléculaire, CNRS, Rue Charles Sadron, F-45071 Orléans Cédex 2, France

Received 2 January 1996
Accepted 10 June 1996

Keywords: DNA; Dynamics; ^{13}C-labeled; ^{13}C NMR; *Lac* operator

Summary

In order to study some internal dynamic processes of the *lac* operator sequence, the ^{13}C-labeled duplex 5'd($C_0G_1C_2T_3C_4A_5C_6A_7A_8T_9T_{10}$)·d($A_{10}A_9T_8T_7G_6T_5G_4A_3G_2C_1G_0$)3' was used. The spreading of both the H1' and C1' resonances brought about an excellent dispersion of the ^{1}H1'-^{13}C1' correlations. The spin–lattice relaxation parameters $R(C_z)$, $R(C_{x,y})$ and $R(H_z \rightarrow C_z)$ were measured for each residue of the two complementary strands, except for the 3'-terminal residues which were not labeled. Variation of the relaxation rates was found along the sequence. These data were analyzed in the context of the model-free formalism proposed by Lipari and Szabo [(1982) *J. Am. Chem. Soc.*, **104**, 4546–4570] and extended to three parameters by Clore et al. [(1990) *Biochemistry*, **29**, 7387–7401; and (1990) *J. Am. Chem. Soc.*, **112**, 4989–4991]. A careful analysis using a least-squares program showed that our data must be interpreted in terms of a three-parameter spectral density function. With this approach, the global correlation time was found to be the same for each residue. All the C1'-H1' fragments exhibited both slow ($\tau_s = 1.5$ ns) and fast ($\tau_f = 20$ ps) restricted libration motions ($S_s^2 = 0.74$ to 1.0 and $S_f^2 = 0.52$ to 0.96). Relaxation processes were described as governed by the motion of the sugar relative to the base and in terms of bending of the whole duplex. The possible role played by the special structure of the AATT sequence is discussed. No evident correlation was found between the amplitude motions of the complementary residues. The 5'-terminal residues showed large internal motions ($S^2 = 0.5$), which describe the fraying of the double helix. Global examination of the microdynamical parameters S_f^2 and S_s^2 along the nucleotide sequence showed that the adenine residues exhibit more restricted fast internal motions ($S_f^2 = 0.88$ to 0.96) than the others, whereas the measured relaxation rates of the four nucleosides in solution were mainly of dipolar origin. Moreover, the fit of both $R(C_z)$ and $R(Hz \rightarrow C_z)$ experimental relaxation rates using an only global correlation time for all the residues, gave evidence of a supplementary relaxation pathway affecting $R(C_{x,y})$ for the purine residues in the (5'→3') G_4A_3 and $A_{10}A_9T_8T_7$ sequences. This relaxation process was analyzed in terms of exchange stemming from motions of the sugar around the glycosidic bond on the millisecond time scale. It should be pointed out that these residues gave evidence of close contacts with the protein in the complex with the *lac* operator [Boelens et al. (1987) *J. Mol. Biol.*, **193**, 213–216] and that these motions could be implied in the *lac*-operator–*lac*-repressor recognition process.

Introduction

The sequence dependence of the structure and internal dynamics of oligodeoxynucleotides is of considerable importance in understanding the mechanism of recognition of specific DNA sequences by proteins such as repressors, restriction endonucleases and RNA polymerase or other ligands.

NMR relaxation experiments can, as a rule, provide a detailed description of nucleic acid dynamics. This is often accomplished using T_1, $T_{1\rho}$ and NOE experiments, which are related to the spectral density functions describing such motions at different frequencies. For each nucleus, these data depend on the magnitude and the rate of the relative motions of all its surrounding nuclei. The use of ^{13}C-NMR relaxation parameters for dynamical analysis is attractive because the C-H bond distance is nearly constant. Thus, the interpretation of the relaxation para-

*To whom correspondence should be addressed.

meters is reduced to the analysis of ^{13}C-^{1}H vectors as a function of time. In order to increase the low natural abundance of the isotope, selectively ^{13}C-labeled molecules are required.

In a previous paper we presented an approach of the internal dynamic processes of the dodecamer d(CGCAAA*TTT*GCG)$_2$, selectively labeled on the three central thymines (Gaudin et al., 1995). Experimental spin–lattice relaxation rates were simulated by computing the effect of local and internal motions of the vector C1'-H1' on the density functions, and two models for the internal mobility of the base pairs and of the sugars relative to the bases in DNA were presented for the three thymines. In order to complete this first analysis we present now an NMR investigation of the C1'-H1' dynamic processes in the undecamer consisting of the complementary strands 5'd(*CGCTCACAAT*T) and 5'd(*AATTGTGAGCG*). This duplex is non-selfcomplementary and allows comparison of the dynamic processes of the two strands. Moreover, it belongs to the lactose-operator sequence and was selectively ^{13}C-labeled at the C1' position of 20 nucleotides. It is a good candidate for a forthcoming study of dynamic processes in DNA selectively complexed with a protein. The aim of this paper is to look for any sequence effect in dynamic processes and any correlation with the residues implied in the specific recognition process of the *lac* operator by the *lac* repressor.

Materials and Methods

Sample preparation

The [1'-^{13}C]-dT, -dC, -dA, and -dG and the required [1'-^{13}C]-labeled oligodeoxynucleotides 5'd(*CGCTCACAAT*T) and 5'd(*AATTGTGAGCG*) were prepared as previously described (Chanteloup and Beau, 1992). Oligonucleotide solutions were passed through a chelex-100 column to remove paramagnetic impurities and adjusted to pH 7.0, then lyophilized from D_2O and dissolved in D_2O containing 0.125 M NaCl. The NMR sample (0.735 mM double strand) was degassed and kept in a sealed tube under argon atmosphere. The oligonucleotide concentrations were determined by using optical measurements with respective molar extinction coefficients of 115 700 and 112 000 $M^{-1}cm^{-1}$ at 260 nm. The two-strand mixture (1:1) was verified by measuring the methyl-area resonances in ^{1}H NMR spectra. Deuterium oxide (D_2O) and (methyl sulfoxide)-d_6 (DMSO-d_6) were purchased from Euriso-top (Saint-Aubin, France).

NMR spectroscopy

All NMR experiments were carried out at 22 °C on a 500 MHz Bruker AMX500 spectrometer operating in the 'reverse' mode and processed on an X32 computer. The relaxation rates of $R(C_z)$, $R(C_{x,y})$ and $R(H_z \rightarrow C_z)$ were measured following the pulse sequences described before (Kay et al., 1992; Peng and Wagner, 1992). Heteronuclear spin-lock and proton irradiation during the relaxation period were used in order to decouple the cross-relaxation pathways (during the relaxation experiments), and to approach monoexponential behaviour as closely as possible (Boyd et al., 1990; Palmer et al., 1991; Peng and Wagner, 1992). T_1 and $T_{1\rho}$ experimental values were measured for relaxation delays of 1.6 s between transient periods. The heteronuclear NOE value was tested with several values of the cross- relaxation delay (1, 1.5, 2, and 3 s) and of the relaxation delay (1.5, 2, 3, and 5 s); finally, values of 1.5 s for the cross-relaxation delay and 2 s for the relaxation delay were used. All data sets were recorded as 256×1024 real matrices. For each t_1 value, 64 and 128 scans were collected for the $R(C_z)$, $R(C_{x,y})$ and $R(H_z \rightarrow C_z)$ measurements, respectively. The heteronuclear NOE values were measured for a cross-relaxation delay of 1500 ms. The matrix was zero-filled along the t_1-axis and multiplied by a sinus function, shifted by $\pi/4$. The Fourier-transformed spectra were baseline-corrected in both dimensions with a second-order polynomial fitting. The cross-peak volumes were calculated with the integration routines of the UXNMR software package on a Bruker Aspect X32 workstation.

Relaxation rate measurements

T_1 and $T_{1\rho}$ experiments were measured using 10 points (Fig. 1). Curve fitting was performed using a nonlinear least-squares program (Lancelot, 1977) to minimize the

TABLE 1
EXPERIMENTAL SPIN-LATTICE RELAXATION RATES COMPUTED FROM T_1, $T_{1\rho}$ AND NOE FOR TWO COMPLEMENTARY UNDECAMERS CONTAINING THE *lac* OPERATOR SEQUENCE

Nucleoside	Spin–lattice relaxation rate (s^{-1})		
	$R(C_z)$	$R(C_{x,y})$	$R(H_z \rightarrow C_z)$
C_0	2.10 ± 0.12	10.30 ± 0.45	0.294 ± 0.059
G_1	2.64 ± 0.07	18.29 ± 0.58	0.125 ± 0.024
C_2	2.22 ± 0.07	15.50 ± 0.69	0.167 ± 0.092
T_3	2.31 ± 0.12	16.23 ± 1.03	0.139 ± 0.029
C_4	2.44 ± 0.11	13.78 ± 0.40	0.375 ± 0.107
A_5	2.73 ± 0.18	19.26 ± 1.30	0.089 ± 0.050
C_6	2.35 ± 0.11	15.85 ± 0.54	0.165 ± 0.046
A_7	2.78 ± 0.09	20.02 ± 0.76	0.139 ± 0.032
A_8	2.68 ± 0.11	19.19 ± 0.72	0.134 ± 0.060
T_9	2.63 ± 0.10	18.12 ± 0.71	0.105 ± 0.057
C_1	2.14 ± 0.11	13.50 ± 0.50	0.091 ± 0.026
G_2	2.50 ± 0.20	15.12 ± 0.70	0.231 ± 0.07
A_3	2.64 ± 0.18	20.86 ± 0.35	0.152 ± 0.061
G_4	2.27 ± 0.10	16.89 ± 0.80	0.153 ± 0.045
T_5	2.35 ± 0.03	15.99 ± 0.35	0.153 ± 0.062
G_6	2.64 ± 0.07	18.29 ± 0.58	0.125 ± 0.024
T_7	2.36 ± 0.10	16.18 ± 1.00	0.136 ± 0.065
T_8	2.35 ± 0.11	15.45 ± 1.15	0.135 ± 0.024
A_9	2.78 ± 0.15	21.75 ± 1.26	0.146 ± 0.015
A_{10}	2.25 ± 0.10	14.30 ± 0.46	0.247 ± 0.027

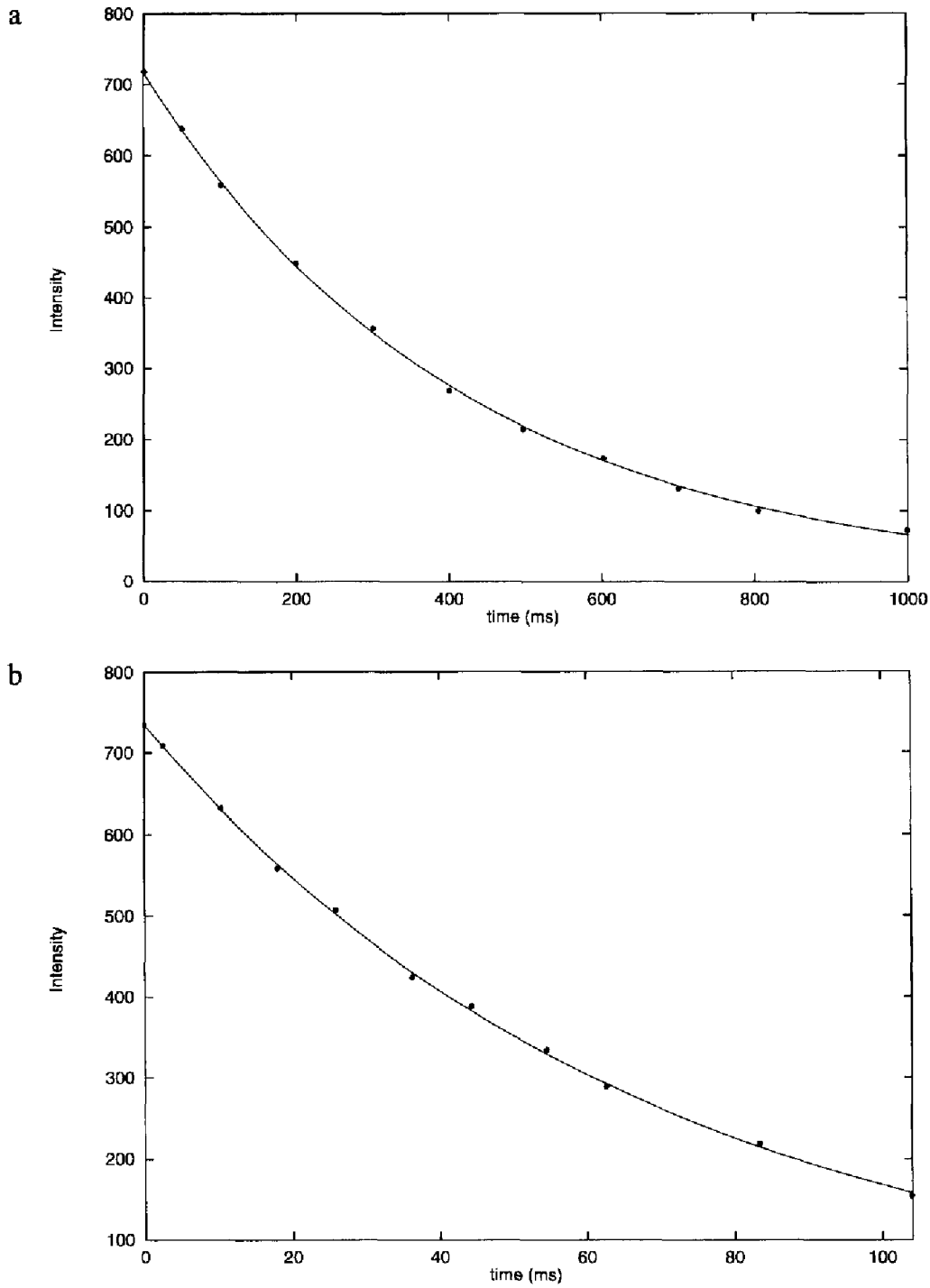

Fig. 1. Examples of relaxation curves resulting from T_1 (a) and $T_{1\rho}$ (b) experiments at 22 °C for the T_5 residue. (a) T_1 fit consisting of 11 points at 0, 50, 100, 200, 300, 400, 500, 600, 700, 800 and 1000 ms. The T_1 fitted value was 419 ± 11 ms in a 90% confidence interval; (b) $T_{1\rho}$ fit consisting of 11 points at 0, 2.6, 10.4, 18.2, 26.0, 36.4, 44.2, 54.6, 62.4, 83.2 and 104.0 ms. The $T_{1\rho}$ fitted value was 68 ± 2 ms in a 90% confidence interval.

χ^2 value. The experimental error was computed using the method previously published (Gaudin et al., 1995). Two series of T_1 and $T_{1\rho}$ measurements were performed. Within experimental errors the measured values were the same.

NOE values which resulted from differences between two volume measurements were more spoiled. Nevertheless, accurate values of the $R(H_z \rightarrow C_z)$ relaxation rates are essential to undertake a fast dynamical processes investigation. In order to reduce the experimental error, six series of NOE experiments were performed. Each error volume measurement was evaluated as depending on the noise in the investigated 2D region of the map. The six NOE values gave similar results within the experimental error for each residue. Their averages were calculated and are given as the measured NOE values in Table 1.

Dynamic parameter computations

The global or internal (τ_g, τ_i, τ_s, τ_f) correlation times, the diffusion coefficients and the order parameters were computed by using a nonlinear least-squares program. The dynamic parameters were evaluated by running the computation with all the combinations of the three relaxation rate values taken as $R+\Delta R$ and $R-\Delta R$. The averages of these data, and the errors evaluated as the root mean square of all the values obtained for the different combinations, are given in Tables 3–5.

Results

The spreading of both the H1' and C1' resonances brought about an excellent dispersion of the ^{1}H1'-^{13}C1' correlations (Fig. 2). Their assignments were published previously (Lancelot et al., 1993) and are used here. The experimental relaxation rates $R(C_z)$, $R(C_{x,y})$ and $R(H_z \rightarrow C_z)$ of each residue are given in Table 1. The $R(C_z)$ values varied from 2.1 to 2.8 s^{-1}, the $R(C_{x,y})$ from 10.3 to 21.8 s^{-1}, and the $R(H_z \rightarrow C_z)$ values from 0.09 to 0.38 s^{-1}.

The model-free formalism of Lipari and Szabo (1982a,b) used for the interpretation of relaxation data makes the assumption that overall and internal motions contribute independently to the reorientational time correlation function of the ^{13}C1'-H1' vector and that internal motions occur on a much faster time scale than the global rotation of the molecule. For an isotropically tumbling molecule:

$$J(\omega) = 2/5\,[S^2\tau_g/(1+\omega^2\tau_g^2) + (1-S^2)\tau_e/(1+\omega^2\tau_e^2)] \quad (1)$$

with $\tau_e^{-1} = \tau_g^{-1} + \tau_i^{-1}$.

The order parameter S^2 describes the relative amplitude of internal motions and ranges from 0 to 1. In the limit of very fast internal motion, $\tau_i \ll \tau_g$, the effective correlation time τ_e becomes equal to τ_i, and consequently is relative to the rate of the internal dynamics. Under these conditions Eq. 1 becomes:

$$J(\omega) = 2/5\,[S^2\tau_g/(1+\omega^2\tau_g^2) + (1-S^2)\tau_i/(1+\omega^2\tau_i^2)] \quad (2)$$

Table 2 gives the τ_g, τ_i and S^2 values obtained using the model-free parameters. Along the sequence, τ_g changes from 3.7 to 4.4 ns and S^2 from 0.50 to 0.95, while τ_i is in the range of 10–80 ps. The relaxation rates are not very sensitive to motions in the picosecond range. Consequently, the τ_i relative incertitude was much greater (17–100%) than the τ_g (3–8%) and the S^2 (2–6%) incertitudes. With-

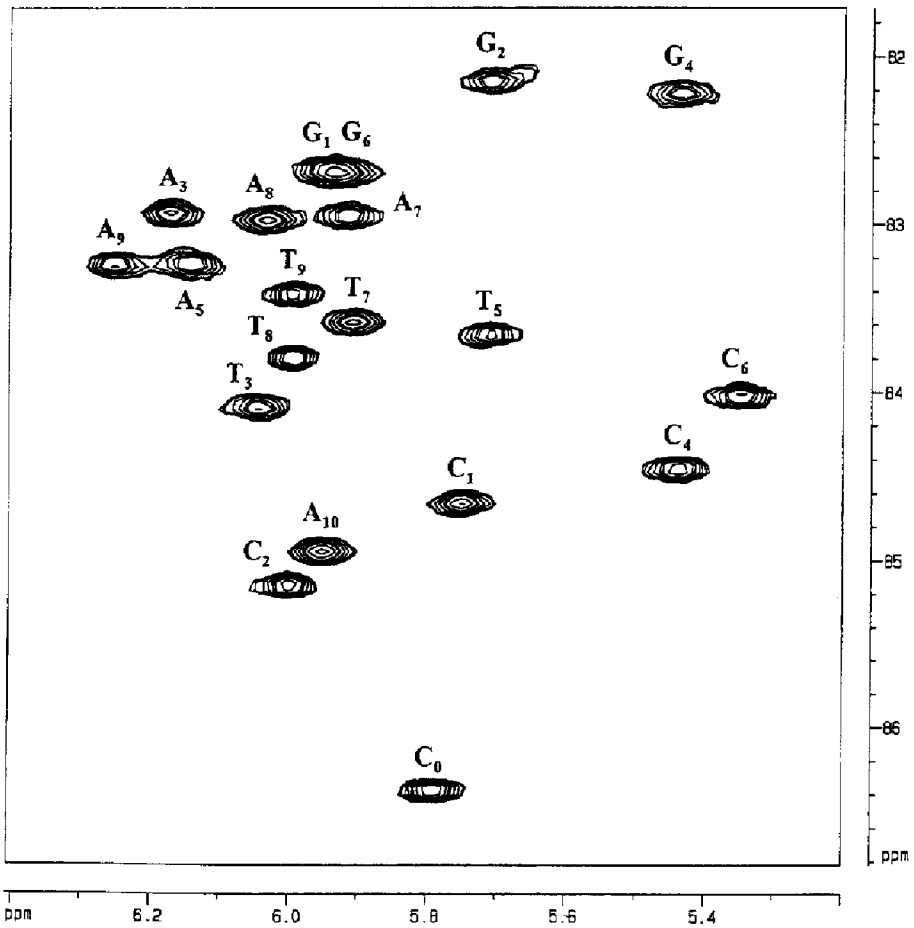

Fig. 2. 500 MHz 2D pure phase absorption ^{13}C-^{1}H HMQC spectrum at 22 °C of the ^{13}C1'-labeled duplex: 5'd($C_0G_1C_2T_3C_4A_5C_6A_7A_8T_9T_{10}$)·d($A_{10}A_9T_8T_7G_6T_5G_4A_3G_2C_1G_0$)3'. The residues T_{10} and G_0 are unlabeled.

TABLE 2
EXPERIMENTAL SPIN–LATTICE RELAXATION RATES COMPUTED FROM T_1, T_2 AND NOE VALUES FOR SELECTIVELY C1'-ENRICHED NUCLEOSIDES IN DMSO-d_6 AT 20 °C

Nucleoside	Spin–lattice relaxation rate (s^{-1})		
	$R(C_z)$	$R(C_{x,y})$	$R(H_z \rightarrow C_z)$
2'-Deoxy-N^6-benzoyl-adenosine	2.34 ± 0.03	2.90 ± 0.04	1.30 ± 0.01
2'-Deoxy-N^2-phenoxyacetyl-guanosine	2.98 ± 0.07	3.30 ± 0.06	1.42 ± 0.01
2'-Deoxy-thymidine	2.10 ± 0.04	2.44 ± 0.02	1.27 ± 0.01
2'-Deoxy-N^2-benzoyl-cytidine	2.53 ± 0.04	3.46 ± 0.05	1.43 ± 0.01

out taking into account the terminal residue values, we note a large heterogeneity along the sequence, which could not be explained by the uncertainty in the data.

Before drawing a general conclusion from these results, the influence of the asymmetric shape of DNA needs to be tested. A careful computation of the spin–lattice relaxation rates of C1' must consider all possible orientations of the C1'-H1' vector as well as the global shape of DNA. The duplex can be modeled by a cylinder with a length of 11 times 3.4 Å (L = 37.4 Å) and a diameter of 20.5 Å (Eimer et al., 1990). Using the relations published by Tirado and Garcia de la Torre (1979,1980), we used the ratio $D_\parallel/D_\perp = 2.0$ between the translational $D_\parallel$ and rotational $D_\perp$ diffusion coefficient. Using the solution structure data (Gincel et al., 1994), we computed a θ angle variation between 62° and 88°. The final diffusion coefficient values were adjusted to give the best fit of the experimental data by computing the spectral density J(ω) with the relation:

$$J(\omega) = S^2/4\,[(3\cos^2\theta - 1)\,j(\tau_1) + 3\cos^2\theta \sin^2\theta\, j(\tau_2) + 3/4\sin^2\theta\, j(\tau_3)] + (1-S^2)\,j(\tau_1) \quad (3)$$

with $j(\tau) = 2/5\tau/(1+\omega^2\tau^2)$, $\tau_1 = 6D_\parallel$, $\tau_2 = D_\parallel + 5D_\perp$ and $\tau_3 = 4D_\parallel + 2D_\perp$.

As already noted by using the two-parameter model-free formalism, the data are not fitted well with a single value of $D_\parallel$ and $D_\perp$. A good fit needs 19% variation of the diffusion coefficient along the sequence, whereas the diffusion constants $D_\parallel$ and $D_\perp$ should be the same for every nucleotide along the sequence. So the simple form of the equation turns out to be insufficient to agree with the whole set of experimental data. Before bringing in a more sophisticated spectral density function, the relative contribution of each relaxation process requires estimation.

Are the relaxation rates only governed by spin–lattice relaxation processes?

Table 1 shows that $R(C_{x,y})$ relaxation rates of the adenines and to a lesser extent their $R(C_z)$ values, showed the greatest variations as compared to the average behaviour of the nucleotides, except the terminal residues. In order to investigate the possible difference in the relaxation pathways for adenine residues as compared to the other nucleotides, we have measured the spin–lattice relaxation rates $R(C_z)$, $R(C_{x,y})$ and $R(H_z \rightarrow C_z)$ of the four protected nucleosides in DMSO-d_6 at 20 °C (Table 2).

For each nucleoside, the $R(C_z)$ value was about half the $R(H_z \rightarrow C_z)$ value, indicating that the process is mainly of dipolar origin. This conclusion is similar to that already published for 1,3-dimethyl thymine in $CDCl_3$ (Williamson and Boxer, 1988). Moreover, the $R(C_{x,y})$ value is about the same as the $R(C_z)$ values expected for ^{13}C spin–lattice relaxation rates in small molecules, indicating the lack of supplementary relaxation processes, such as exchange. It can be pointed out that T_2 measurements gave a greater R_2 value for cytidine than for the three other nucleosides. This difference decreased by irradiating the $^{13}C1'$ resonance during the cross-relaxation delay. In fact, the quadrupolar of nitrogen N1 or N9 is higher for cytosine (Kuroda et al., 1985) than for the other bases (Schempp and Bray, 1971). Consequently, this supplementary relaxation pathway was assigned as a scalar relaxation process of the second kind. It can be pointed out that the efficiency of this process decreases with the global correlation time of the molecule. Although a τ_g value of 10 ps (for cytidine) led to $R_{SC\,II}$ in the range of s^{-1}, a global correlation time of 4 ns drastically decreases the $R_{SC\,II}$ value to 2.5×10^{-3} s^{-1}. Consequently, scalar relaxation cannot be an efficient relaxation pathway for the C1' nucleus in oligonucleotides. Moreover, ^{13}C spin-lock during the relaxation delay destroyed any scalar spin-coupling effect.

Other relaxation pathways which could be efficient need to be estimated. The chemical shift anisotropy relaxation process has already been calculated (Gaudin et al., 1995) to contribute only 2% to the total relaxation. As a result, great care was taken in sample preparation to eliminate the paramagnetic impurities, such as cations or oxygen. Since the relaxation rates are similar for the four free nucleosides in solution, and the scalar relaxation process as well as the chemical shift anisotropy relaxation process are negligible for C1' nuclei in oligonucleotides, differences in $R(Cz_{x,y})$ between the residues can only be induced by supplementary slow dipole–dipole relaxation processes or by chemical exchange.

Additional relaxation pathways induced by slow motions

When fast and slow internal motions coexist, the correlation function becomes biexponential, and the expression of the spectral density function consistent with the available relaxation data is given by Eq. 4 (Clore et al., 1990):

$$J(\omega) = 2/5\,[S_f^2 S_s^2\, j(\tau_g) + (1-S_f^2)\,j(\tau_f) + S_f^2(1-S_s^2)\,j(\tau_s)] \quad (4)$$

with $j(\tau) = \tau/(1+\omega^2\tau^2)$.

S_f^2 and S_s^2 are the generalized order parameters of the fast (picosecond time scale) and slow (nanosecond time

scale) motions, and τ_f and τ_s are the corresponding correlation times. A best fit of the experimental relaxation rates was obtained by using a global correlation time of 4.5 ns and by optimizing τ_s and τ_f to 1.5 ns and 20 ps, respectively. The corresponding amplitude parameters are given in Table 3.

Slow motions

All the residues, except the terminal C_0, exhibited an additional slow motion on the nanosecond time scale (1.5 ns) with an order parameter S_s^2 in the range of 0.81 to 1.0. These slow motions with weak amplitudes could be involved in the global bending of DNA.

Another interesting feature is that the terminal residues C_0 exhibited a larger slow motion ($S_s^2 = 0.74$) than the terminal residue A_{10} of the other end ($S_s^2 = 0.91$). Such different behaviour between the two complementary strands has been previously observed (Koning et al., 1991) by computing the root mean square of the atom C1' for the 180-ps trajectory of the duplex d(GCGTTGCG)·d(CGCAACGC). An analysis of the dynamical behaviour of axis base pairs, intra-base pairs, inter-base pairs and axis-junction parameters for $d(CGCGAATTCGCG)_2$ (Swaminathan et al., 1991) showed a rapid oscillatory motion on the picosecond time scale, with an apparent slower motion (several hundred ps) superimposed for all nucleotides, which is more important toward the ends of the helix.

A 1-ns molecular dynamics simulation on the $d(CGCGAATTCGCG)_2$ duplex (McConnell et al., 1994) showed that after an equilibration period, the MD structure resided for ~300 ps in a first form similar to canonical B-form DNA, and then made a distinct transition to a new form, where it remained for 180 ps. After that the dynamical structure switched to a third form, where it resided until the end of the run. These data are indicative of motions whose period is in the range of several hundreds of picoseconds. Furthermore, the bending analysis of MD simulation (Young et al., 1994) shows a 500-ps trajectory which denotes a variation of the bending magnitude up to 45°. These large variations of the oligonucleotide bending on a long time scale could be at the origin of the observed slow restricted motion evaluated by S_s^2.

Fast motions

All residues exhibit fast internal motions on a time scale of 20 ps. The variation of the corresponding order parameter S_f^2 is depicted in Table 3. The origin of the $^{13}C1'$ relaxation was previously analyzed (Gaudin et al., 1995) with respect to the motions of the sugar around the C1'-N1 (C1'-N9) bond. A two-state jump model between the *anti* and *syn* conformations, with P(*anti*)/P(*syn*) = 91/9, or a restricted rotation model with $\Delta\chi = 28°$, fitted well with a fast (16 ps) restricted motion ($S^2 = 0.83$) of the C1'-H1' vector. For the strand d(CGCTCACAATT) the value of S_f^2 was 0.71 ± 0.02 for all the pyrimidines, except for the terminal residue C_0 and for T_9 in the sequence AAT. The purines exhibited more restricted motions ($S_f^2 = 0.85$ to

TABLE 3

GLOBAL TUMBLING AND INTERNAL MOTION PARAMETERS OBTAINED WITH THE TWO-PARAMETER MODEL-FREE FORMALISM

Nucleoside	Parameters						
	τ_g [a] (ns)	S^2 [a]	τ_i [a] (ns)	θ [b] (°)	$D_\parallel$ [b] (10^7 s^{-1})	S^2 [b]	τ_i [b] (ns)
C_0	3.7 ± 0.3	0.50 ± 0.03	0.04 ± 0.01	85	6.3 ± 0.5	0.49 ± 0.03	0.015 ± 0.004
G_1	4.0 ± 0.1	0.86 ± 0.02	0.01 ± 0.02	85	5.7 ± 0.2	0.85 ± 0.02	0.003 ± 0.006
C_2	4.2 ± 0.3	0.70 ± 0.04	0.02 ± 0.03	80	5.6 ± 0.4	0.69 ± 0.04	0.007 ± 0.010
T_3	4.1 ± 0.3	0.74 ± 0.03	0.02 ± 0.01	76	5.7 ± 0.5	0.73 ± 0.06	0.002 ± 0.019
C_4	4.2 ± 0.3	0.61 ± 0.05	0.07 ± 0.03	76	5.7 ± 0.5	0.60 ± 0.05	0.025 ± 0.012
A_5	4.0 ± 0.3	0.90 ± 0.03	0.02 ± 0.03	77	5.8 ± 0.4	0.88 ± 0.03	0.002 ± 0.004
C_6	4.1 ± 0.2	0.73 ± 0.03	0.02 ± 0.02	72	5.8 ± 0.3	0.72 ± 0.03	0.008 ± 0.006
A_7	4.1 ± 0.1	0.92 ± 0.02	0.03 ± 0.03	64	5.9 ± 0.2	0.91 ± 0.02	0.007 ± 0.013
A_8	4.1 ± 0.2	0.89 ± 0.03	0.01 ± 0.05	67	5.9 ± 0.3	0.87 ± 0.03	0.003 ± 0.018
T_9	4.0 ± 0.2	0.86 ± 0.03	0.01 ± 0.03	65	6.1 ± 0.3	0.85 ± 0.03	0.001 ± 0.012
C_1	3.8 ± 0.2	0.67 ± 0.02	0.01 ± 0.01	85	6.1 ± 0.3	0.66 ± 0.02	0.001 ± 0.003
G_2	3.8 ± 0.3	0.74 ± 0.04	0.01 ± 0.03	80	5.9 ± 0.5	0.70 ± 0.04	0.015 ± 0.010
A_3	4.4 ± 0.2	0.92 ± 0.03	0.01 ± 0.03	76	5.3 ± 0.2	0.90 ± 0.03	0.007 ± 0.010
G_4	4.3 ± 0.2	0.75 ± 0.03	0.02 ± 0.02	76	5.5 ± 0.3	0.73 ± 0.03	0.008 ± 0.006
T_5	4.1 ± 0.2	0.75 ± 0.03	0.02 ± 0.02	81	5.7 ± 0.2	0.74 ± 0.03	0.007 ± 0.008
G_6	4.0 ± 0.1	0.86 ± 0.02	0.01 ± 0.02	62	5.7 ± 0.2	0.85 ± 0.02	0.003 ± 0.006
T_7	4.0 ± 0.3	0.75 ± 0.03	0.01 ± 0.02	70	5.9 ± 0.4	0.74 ± 0.03	0.004 ± 0.009
T_8	3.9 ± 0.3	0.73 ± 0.03	0.01 ± 0.01	84	5.9 ± 0.4	0.72 ± 0.02	0.005 ± 0.003
A_9	4.3 ± 0.3	0.95 ± 0.03	0.08 ± 0.05	88	5.4 ± 0.3	0.95 ± 0.03	0.002 ± 0.002
A_{10}	4.1 ± 0.2	0.64 ± 0.02	0.04 ± 0.01	88	5.6 ± 0.3	0.63 ± 0.02	0.015 ± 0.002

[a] Using the general Lipari–Szabo expression.

[b] Assuming the global shape of the double helix as a cylinder ($D_\parallel/D_\perp = 2.0$) and an internal motion. θ is the polar angle of the vector C1'-H1' (see text).

0.92). For the complementary strand d(AATTGTGAGC) the value of S_f^2 was 0.73 ± 0.02 for all residues, except for the flanking terminal residues C_1 and A_9, as well as A_3 and G_6. This value is in the range of the order parameter computed for the three thymines of the self-complementary duplex d(CGCAAA*TTT*GCG) (Gaudin et al., 1995) and could indicate a restricted rotation of the sugar moiety about the glycosidic bond in the range of 30°. The terminal residues exhibit a clearly increased mobility. This effect is more pronounced for the extremity implicating C_0 and G_0 ($S_f^2 = 0.52$ for C_0) of the duplex than for the other one ($S_f^2 = 0.67$ for A_{10}). These data indicate larger motions of the extremities, which reflect their fraying. Conversely, the adenine residues present strongly restricted amplitude motions with S_f^2 ranging from 0.88 to 0.96.

Exchange relaxation

NMR chemical exchange processes are efficient when the exchange time scale is in the range of microseconds to seconds. Consequently, only components implicating a low frequency are modified and the term R_{ex} must be added to the spin–lattice relaxation rates $R(C_{x,y})$. In order to compute the possible $R_{ex}(C_{x,y})$ contribution for each nucleoside, we evaluated firstly the global correlation time of the *lac* operator. The global correlation time was computed to give the best fit of the three relaxation rates for each residue, except for those at the termini and the A_3, G_4 and A_9 residues, which presented the largest deviation of τ_g in the two-parameter model-free formalism analysis (Table 2).

Using this τ_g value (4.1 ns), S^2 and τ_i were adjusted to give the best fit of $R(C_z)$ and $R(H_z \rightarrow C_z)$ for each residue. Table 5 gives the S^2 and τ_i values computed for each residue and the difference between R_{exp} and R_{comp} for the three relaxation rates. On the one hand, $R(C_z)$ and $R(H_z \rightarrow C_z)$ were well fitted for all the residues. On the other hand, $R(C_{x,y})_{exp} - R(C_{x,y})_{comp}$ exhibited negative differences for the terminal residue C_0 and the flanking terminal residues C_1. These negative values may reflect the lack of validity of this relaxation model for the terminal or flanking terminal residues for which fraying motions must be taken into account. Moreover, the residues A_3, G_4 and A_9 exhibited a positive difference in the range of 1 to 3 s^{-1}. These differences are without the uncertainty of the data and reflect a supplementary relaxation pathway involving a time scale much longer than 1 ns, as expected in efficient chemical exchange processes.

For a two-step exchange process, the contribution of exchange to $R(C_{x,y})$ is related by (Deverell et al., 1970; Bleich and Glasel, 1978; Blackledge et al., 1983):

$$R_{ex} = (\Delta\omega)^2 P_1 P_2 \tau_{ex} / (1 + \omega_1^2 \tau_{ex}^2) \qquad (5)$$

where P_1 and P_2 are the populations of the two conformers, $\Delta\omega$ the resonance frequency difference between the exchanging sites and ω_1 the equivalent frequency of the applied rf field.

The $^{13}C1'$ resonances are spread out over 4 ppm in the *lac* operator. Using this value as the scale of chemical shift change, we estimated that a $\Delta\nu$ value in the range of 40 Hz may reflect the conformational changes at 125 MHz. Thus, a population value P_1 in the range of 0.5 ($P_2 = 0.5$), a spin-lock value of 1 kHz, and τ_{ex} in the range of 160 µs, give $R_{ex} = 1.2$ s^{-1}. Although the temperature dependence of the R(Cx,y) relaxation rates could yield supplementary information on exchange processes, the excessive acquisition time required for such a large number of 2D maps precluded this analysis.

TABLE 4
ORDER PARAMETERS FOR THE FAST (S_f^2) AND SLOW (S_s^2) MOTIONS COMPUTED FROM THE EXPERIMENTAL RELAXATION RATES USING THE FOUR-PARAMETER MODEL-FREE FORMALISM

Nucleoside	Order parameter	
	S_f^2	S_s^2
C_0	0.52 ± 0.02	0.74 ± 0.07
G_1	0.85 ± 0.01	0.94 ± 0.03
C_2	0.70 ± 0.02	0.96 ± 0.04
T_3	0.73 ± 0.03	0.96 ± 0.07
C_4	0.68 ± 0.01	0.81 ± 0.05
A_5	0.88 ± 0.03	0.95 ± 0.08
C_6	0.73 ± 0.02	0.94 ± 0.05
A_7	0.92 ± 0.02	0.96 ± 0.04
A_8	0.88 ± 0.02	0.96 ± 0.05
T_9	0.84 ± 0.02	0.94 ± 0.05
C_1	0.63 ± 0.01	0.91 ± 0.06
G_2	0.72 ± 0.02	0.87 ± 0.08
A_3	0.93 ± 0.02	1.00 ± 0.05
G_4	0.75 ± 0.02	1.00 ± 0.05
T_5	0.74 ± 0.01	0.94 ± 0.02
G_6	0.85 ± 0.01	0.94 ± 0.03
T_7	0.74 ± 0.03	0.94 ± 0.06
T_8	0.71 ± 0.03	0.91 ± 0.07
A_9	0.96 ± 0.03	1.00 ± 0.06
A_{10}	0.67 ± 0.01	0.91 ± 0.05

The global and internal correlation times were $\tau_g = 4.25$ ns, $\tau_s = 1.5$ ns and $\tau_i = 20$ ps for all residues.

Discussion

A good fit of the $R(C_z)$, $R(C_{x,y})$ and $R(H_z \rightarrow C_z)$ values has been obtained by using two different analyses. In the first one a global correlation time of 4.25 ns was computed, indicating that every residue, except A_3, G_4 and A_9, was subjected to internal motions containing both fast and slow components. One striking feature is that all the adenine residues showed strongly restricted amplitudes for fast motions. The second analysis involved exchange processes implicating the three residues A_3, G_4, A_9, and likely A_{10}. In fact, it should be pointed out that the $R(C_{x,y})$ value of A_{10} is 4 s^{-1} greater than the corresponding value of C_0.

TABLE 5
INTERNAL MOTION PARAMETERS

Nucleoside	Internal motion parameters		Relaxation rates (s^{-1})		
	S^2	τ_i (ps)	$\Delta R(C_z)$	$\Delta R(C_{x,y})$	$\Delta R(H_z \rightarrow C_z)$
C_0	0.55 ± 0.06	43 ± 09	0.04 ± 0.12	−1.80 ± 0.45	0.002 ± 0.059
G_1	0.88 ± 0.03	9 ± 19	0.03 ± 0.07	−0.54 ± 0.58	0.004 ± 0.024
C_2	0.69 ± 0.07	18 ± 24	0.06 ± 0.07	0.59 ± 0.69	0.018 ± 0.092
T_3	0.74 ± 0.05	15 ± 09	0.04 ± 0.12	0.31 ± 1.03	0.002 ± 0.029
C_4	0.61 ± 0.09	67 ± 16	0.05 ± 0.11	0.22 ± 0.40	−0.009 ± 0.107
A_5	0.93 ± 0.08	17 ± 94	−0.03 ± 0.18	−0.65 ± 1.30	−0.039 ± 0.050
C_6	0.74 ± 0.05	23 ± 14	0.05 ± 0.11	−0.04 ± 0.54	0.004 ± 0.046
A_7	0.93 ± 0.04	23 ± 15	0.03 ± 0.09	0.25 ± 0.76	0.005 ± 0.032
A_8	0.86 ± 0.08	28 ± 44	−0.01 ± 0.11	0.02 ± 0.72	−0.011 ± 0.060
T_9	0.87 ± 0.04	20 ± 24	0.03 ± 0.10	−0.40 ± 0.71	−0.033 ± 0.057
C_1	0.72 ± 0.04	0.4 ± 7.0	0.04 ± 0.11	−1.77 ± 0.50	0.002 ± 0.026
G_2	0.73 ± 0.09	46 ± 22	0.07 ± 0.20	−0.78 ± 0.70	−0.087 ± 0.073
A_3	0.84 ± 0.07	30 ± 25	0.06 ± 0.18	2.77 ± 0.35	−0.007 ± 0.061
G_4	0.72 ± 0.05	18 ± 13	0.04 ± 0.10	1.43 ± 0.80	0.004 ± 0.045
T_5	0.76 ± 0.05	17 ± 21	0.03 ± 0.03	−0.27 ± 0.35	0.010 ± 0.062
G_6	0.88 ± 0.03	9 ± 19	0.03 ± 0.07	−0.54 ± 0.58	0.004 ± 0.046
T_7	0.77 ± 0.06	10 ± 24	0.06 ± 0.10	−0.20 ± 1.00	0.014 ± 0.065
T_8	0.76 ± 0.04	14 ± 09	0.04 ± 0.11	−0.87 ± 1.15	0.001 ± 0.024
A_9	0.91 ± 0.05	30 ± 40	0.05 ± 0.15	2.27 ± 1.26	0.003 ± 0.015
A_{10}	0.64 ± 0.04	40 ± 06	0.03 ± 0.10	0.30 ± 0.46	0.000 ± 0.027

S^2 and τ_i were obtained by fitting the $R(C_z)$ and $R(H_z \rightarrow C_z)$ relaxation rates with only a global correlation time $\tau_g = 4.1$ ns. ΔR represents the difference $R_{exp} - R_{comp}$ and $\pm \Delta R$ the incertitude on R_{exp}.

Our analysis does not reflect any positive $R(C_{x,y})_{exp} - R(C_{x,y})_{comp}$ value for A_{10}, in spite of the fact that the supplementary motion of the flanking terminal residue decreases its effective global correlation time. Such an exchange process was also underscored by taking the average of the T_2 value of the H2 and H8 protons of adenine in DNA oligonucleotides containing TpA steps (Kennedy et al., 1993). This behaviour was analyzed in terms of motions of the purine base about the glycosidic torsion angle at the TpA junction. This process could also be involved in the *lac* operator and interpreted as being a localized conformational change of the purine residues in the (5'→3') G_4A_5 and the $A_{10}A_9T_8T_7$ sequences.

Although the motion of the sugar moiety around the glycosidic bond was certainly important in our analyses of fast and slow (exchange) motions, it cannot be excluded that other motions afforded efficient relaxation pathways. The curvature of a DNA-carrying adenine tract (dA_n–dT_n) (Wu and Crothers, 1984) may be at the root of the difference in the sequence AATT. Although hydrogen exchange in base pairs occurs only in the range of 1 ms^{-1}, far beyond the picosecond time scale, it is worth noting that such an anomalous behaviour has already been noted in measuring the lifetime of the A–T pair in oligonucleotides containing such tracts (Leroy et al., 1988).

Levitt (1983) reported that the radius of gyration of the dodecamer d(CGCGAATTCGCG) oscillates (24 ps) with an amplitude of 4% of the mean value (13.3 Å). The most significant deformation was bending with a period of 26 ps and an amplitude of 1.18° bending angle per angstrom. This bending motion persisted for the entire trajectory (90 ps) in addition to a significant twisting motion (0.32°/Å). Moreover, an analysis of the bending of oligonucleotides shows that the adenine tract region remains quite straight and that bending occurs at the junctions between adenine and the flanking DNA sequences (Young et al., 1994; Ptaszek et al., 1995). Our data suggest that adenine residues can exhibit fast local motions with smaller amplitude than others. Nevertheless, a combination of this motion with longer-time-scale motions cannot be excluded.

Conclusions

The excellent spreading of the H1'-C1' correlations allowed us to carefully measure the spin relaxation rates of all residues in the half *lac*-operator sequence and to compare the dynamic behaviour of the vectors C1'-H1' for all the ^{13}C-labeled residues. A careful analysis of these data suggested that two types of motions are superimposed: a short-time local fluctuation and a longer-time motion. Similar results were found for adenine residues in the duplex $d(CGCAAATTTGCG)_2$ and they will be reported elsewhere. Two types of analysis of the slow motions fit the experimental data well. The first one gave evidence of slow internal motion in DNA, although its amplitude was weak and almost constant along the sequence, since S^2 is always in the range of 0.87 to 1.0

except for the terminal residue C_0. This analysis implies that all the adenine residues show a strongly restricted amplitude for fast motions, in contrast with the behaviour of their neighboring or paired residues. No mechanical explanation could be given for this. The second analysis, which suggested an exchange process implicating change in the glycosidic angle of the purine in the (5'→3') sequences G_4A_5 and $A_{10}A_9T_8T_7$ on the millisecond time scale seems to give a more convincing explanation for the behaviour of these residues.

In conclusion, our data show fast motions (~20 ps) of the sugars about the glycosidic bond, slow motions (~1 ns) implicating the whole operator, as well as very slow motions (~1 μs) involving the purines in the (5'→3') sequences G_4A_5 and $A_{10}A_9T_8T_7$. It should be noted that these residues were showed to be in close contact with the *lac* repressor protein (Boelens et al., 1987). Such motions could be implicated in the recognition mechanism of the operator by the *lac* repressor. No correlation was observed between the amplitude motions of the complementary nucleotides. Moreover, the two strands showed different mobilities on the 1-ns time scale. This work provides experimental evidence of sequence effects for dynamic processes in DNA. In order to complete our analysis, relaxation rates measurements on the *lac*-operator–*lac*-repressor complex and molecular dynamics oligonucleotides studies are presently carried out in our laboratory.

References

Blackledge, M.J., Brüschweiler, R., Griesinger, C., Schmidt, J.M., Xu, P. and Ernst, R.R. (1993) *Biochemistry*, **32**, 10960–10974.

Bleich, H.E. and Glasel, J.A. (1978) *Biopolymers*, **17**, 2445–2457.

Boelens, R., Scheek, R.M., Van Boom, J.H. and Kaptein, R. (1987) *J. Mol. Biol.*, **193**, 213–216.

Boyd, J., Hommel, U. and Campbell, I.D. (1990) *Chem. Phys. Lett.*, **175**, 477–483.

Chanteloup, L. and Beau, J.M. (1992) *Tetrahedron Lett.*, **33**, 5347–5350.

Clore, G.M., Driscoll, P.C., Wingfield, P.T. and Gronenborn, A.M. (1990a) *Biochemistry*, **29**, 7387–7401.

Clore, G.M., Szabo, A., Bax, A., Kay, L.E., Driscoll, P.C. and Gronenborn, A.M. (1990b) *J. Am. Chem. Soc.*, **112**, 4989–4991.

Deverell, C., Morgan, R.E. and Strange, J.H. (1970) *Mol. Phys.*, **18**, 553–559.

Eimer, W., Williamson, J.R., Boxer, S.G. and Pecora, R. (1990) *Biochemistry*, **29**, 799–811.

Gaudin, F., Paquet, F., Chanteloup, L., Beau, J.-M., Thuong, N.T. and Lancelot, G. (1995) *J. Biomol. NMR*, **5**, 49–58.

Gincel, E., Lancelot, G., Maurizot, J.-C., Thuong, N.T. and Vovelle, F. (1994) *Biochimie*, **76**, 141–151.

Kay, L.E., Nicholson, L.K., Delaglio, F., Bax, A. and Torchia, D.A. (1992) *J. Magn. Reson.*, **97**, 359–375.

Kennedy, M.A., Nuutero, S.T., Davis, J.T., Drobny, G.P. and Reid, B.R. (1993) *Biochemistry*, **32**, 8022–8035.

Koning, T.M.G., Boelens, R., Van der Marel, G.A., Van Boom, J.H. and Kaptein, R. (1991) *Biochemistry*, **30**, 3787–3797.

Kuroda, Y., Fujiwara, Y. and Matsushita, K. (1985) *J. Magn. Reson.*, **62**, 218–225.

Lancelot, G. (1977) *Biochimie*, **59**, 587–596.

Lancelot, G., Chanteloup, L., Beau, J.M. and Thuong, N.T. (1993) *J. Am. Chem. Soc.*, **115**, 599–1600.

Leroy, J.-L., Charretier, E., Kochoyan, M. and Guéron, M. (1988) *Biochemistry*, **27**, 8894–8898.

Levitt, M. (1983) *Cold Spring Harbor Symp. Quant. Biol.*, **47**, 251–262.

Lipari, G. and Szabo, A. (1982a) *J. Am. Chem. Soc.*, **104**, 4546–4559.

Lipari, G. and Szabo, A. (1982b) *J. Am. Chem. Soc.*, **104**, 4559–4570.

McConnell, K.J., Nirmala, R., Young, M.A., Ravishanker, G. and Beveridge, D.L. (1994) *J. Am. Chem. Soc.*, **116**, 4461–4462.

Palmer, A.G., Rance, M. and Wright, P.E. (1991) *J. Am. Chem. Soc.*, **113**, 4372–4380.

Peng, J.W. and Wagner, G. (1992) *J. Magn. Reson.*, **98**, 308–332.

Ptaszek, L.M., Young, M.A., McConnell, K., Ravishanker, G. and Beveridge, D.L. (1995) *J. Biomol. Struct. Dyn.*, **12**, a193.

Schempp, E. and Bray, P.J. (1971) *J. Magn. Reson.*, **5**, 78–83.

Swaminathan, S., Ravishanker, G. and Beveridge, D.L. (1991) *J. Am. Chem. Soc.*, **113**, 5027–5040.

Tirado, M.M. and Garcia de la Torre, J. (1979) *J. Chem. Phys.*, **71**, 2581–2587.

Tirado, M.M. and Garcia de la Torre, J. (1980) *J. Chem. Phys.*, **73**, 1986–1993.

Williamson, J.R. and Boxer, S.G. (1988) *Nucleic Acids Res.*, **16**, 1529–1540.

Wu, H.-M. and Crothers, D.M. (1984) *Nature*, **308**, 509–513.

Young, M.A., Nirmala, R., Srinivasan, J., McConnell, K.J., Ravishanker, G., Beveridge, D.L. and Berman, H.M. (1994) In *Structural Biology: State of the Art 1993: Proceedings of the Eighth Conversation in Biomolecular Stereodynamics* (Eds, Sarma, R.H. and Sarma, M.H.), Adenine Press, Albany, NY, U.S.A., pp. 197–214.